Chapter 9

VARIABLE TERRESTRIAL PARTICLE ENVIRONMENTS DURING THE GALACTIC ORBIT OF THE SUN

Hans J. Fahr
Institut für Astrophysik und Extraterrestrische Forschung, Universität Bonn, Auf dem Hügel 71, 53121 Bonn, Germany
hfahr@astro.uni-bonn.de

Horst Fichtner
Institut für Theoretische Physik IV: Weltraum- und Astrophysik, Ruhr-Universität Bochum, 44780 Bochum, Germany
hf@tp4.rub.de

Klaus Scherer
Institut für Astrophysik und Extraterrestrische Forschung, Universität Bonn, Auf dem Hügel 71, 53121 Bonn, Germany
ks@tp4.rub.de

Olaf Stawicki
Unit for Space Physics, School of Physics, North-West University, Campus Potchefstroom, 2520 Potchefstroom, South Africa
os@tp4.ruhr-unibochum.de

Abstract The effects of variable terrestrial environments of the Sun during its galactic orbit are discussed. Emphasis is put on the energetic particle populations, like pick-up ions, anomalous and galactic cosmic rays. After putting the analysis briefly into the context of the ongoing debate regarding a cosmic ray-terrestrial climate link, we study the structure of the heliosphere in various interstellar environments, particularly in dense clouds of atomic hydrogen. We continue

P. C. Frisch (ed.), Solar Journey: The Significance of our Galactic Environment for the Heliosphere and Earth, 259–279.

with a computation of the energy spectra of both anomalous and galactic cosmic rays for galactic regions located in clouds and/or in galactic spiral arms. In the light of these results we discuss the consequences for the terrestrial and planetary environments, as well as for small solar system bodies.

Keywords: Pick-up ions, energetic neutral atoms, anomalous cosmic rays, dynamic heliosphere

9.1 Introductory Remarks on Cosmic Rays and Climate

The Earth in space represents a thermodynamical non-equilibrium system because it maintains a pronounced exchange of energies with its space environment. The terrestrial electromagnetic and particle radiation environments are changing in time due to solar as well as galactic variabilities. Particularly, the terrestrial climate is a result of a very complicated interactions between open thermodynamic subsystems, like different cloud layers and atmospheric and oceanic circulation patterns on top of a rotating solid body. Consequently, the whole climate system is highly structured with many nonlinear thermal couplings between the lithosphere (i.e. solid Earth crust), the hydrosphere (i.e. the oceans), the atmosphere, and perhaps the biosphere (see, e.g., Cuntz et al., 2003, von Bloh et al., 2003).

It has been argued (Lean and Rind, 1999, Fröhlich and Lean, 2002) that the prime external climate driver on short time scales (Schwabe and Hale cycle, i.e. decades) and on intermediate time scales (Gleisberg cycle and grand activity minima, i.e. centuries and millenia) is solar irradiation, i.e. the integrated electromagnetic energy input into the Earth's upper atmosphere. However, various terrestrial climate drivers, like temperature and cloud coverage of the Earth. correlate well with energetic particle irradiation (Svensmark and Friis-Christensen, 1997, Svensmark, 1998, Svensmark, 2000, Carslaw et al., 2002) on short time scales. For intermediate time scales, the cosmogenic isotope concentration during the Wolf-, Spoerer-, Maunder- and Dalton-Minimum of solar activity indicate an increased cosmic ray flux as recently modelled by Caballero et al. (2004) and Scherer and Fichtner (2004), suggesting that this correlation also holds, because these grand minima coincide with cold periods.

While it cannot yet be determined whether solar or particle irradiation is the prime external climate driver on short and intermediate time scales, this is different for long time scales (galactic arm crossings, i.e. millions of years). For long time scales, the cosmic ray flux varies quasi-periodically during the solar galactic orbit due to enhanced fluxes within spiral arms (Shaviv, 2003), and correlates with long-term temperature variations on Earth (Shaviv and Veizer, 2003). As one should not expect the solar irradiance to correlate with spiral arm crossings, these results are a strong argument for the cosmic rays as climate drivers.

The discussion so far, however, has neither taken into account the variable shielding effect of the heliosphere during a solar galactic orbit nor the permanent presence of an additional energetic particle component, namely anomalous cosmic rays (ACRs). To study both we first investigate the coupling of the interstellar medium (ISM) with the solar wind. An essential role is played by neutral atoms that become ionized within the heliosphere, i.e. the so-called pick-up ions (PUIs), as they have a significant influence on the dynamics of the solar wind and they are the seed population of ACRs. In order to derive the energetic particle spectra at Earth we, secondly, need to include the fluxes of galactic cosmic rays (GCRs), which we estimate from both observations and theoretical considerations. This allows us, finally, to compute the total cosmic ray spectra at Earth.

9.2 The Heliosphere in Different Interstellar Environments

In contrast to the present-day situation, where the heliosphere is located in a dilute ISM (Frisch, 1998, Lallement et al., 2003, Freyberg and Breidtschwerdt, 2003, Breitschwerdt, 2004), a spiral arm crossing provides a dense interstellar environment (DISE). Therefore, we consider typical cases of DISEs in the following. Note, however, that we exclude molecular clouds providing environments of very high interstellar density ($n_H > 1000\,\mathrm{cm}^{-3}$), because the Bonn model (Fahr et al., 2000, Fahr, 2000) we use assumes atomic rather than molecular hydrogen (for the case of molecular clouds see Yeghikyan and Fahr, 2004a). The computations are performed using the five-fluid Bonn model that describes the dynamics of the heliosphere in the presence of solar wind and interstellar protons, interstellar hydrogen, PUIs, ACRs, and GCRs, all of which are mutually interacting (Fahr et al., 2000). The PUIs behave thermodynamically as an individual fluid, which is convected with the solar wind. In turn, the solar wind gets decelerated by momentum loading from these suprathermal particles influencing the compression ratios of the termination shock (TS). Depending on the local strength of the TS, a certain fraction of PUIs is injected at the TS into the process of diffusive shock acceleration, thereby constituting the local ACR source.

9.2.1 The Physics in the Bonn model

In the following we briefly describe the dynamical and thermodynamical coupling of low- and high-energy plasma components as modelled in the Bonn code. The first-order interaction of the solar wind with the interstellar plasma is a hydrodynamic proton-proton interaction. In addition to protons, however, also interstellar H-atoms are flying into the heliosphere, which upon ionization in the region of the supersonic solar wind produce H-pick-up ions (PUIs). Due to effective pitch-angle scattering, they are rapidly isotropized in velocity space and are comoving with the solar wind, thereby representing a keV-energetic ion load of the expanding solar wind. These PUIs are treated in the Bonn model as an additional ion fluid, separated from the solar wind proton fluid by its number density and its pressure. A certain fraction of these PUIs can be injected into the Fermi-1 diffusive acceleration process at the termination shock (Chalov and Fahr, 1997) and act as a seed for the ACR population, which in the multifluid model is also treated by its relevant moment, i.e. the energy density or pressure. This high energy fluid interacts with the solar wind plasma flow via its pressure gradient and, for instance, decelerates it in the region near and upstream of the termination shock, forming a precursor. For stationary conditions the physics in this precursor for the convected low energy plasma species is treated by the following continuity equations (Chalov and Fahr, 1994, Chalov and Fahr, 1995, Chalov and Fahr, 1997, Zank, 1999):

$$\nabla \cdot (\rho_i \vec{u}) = Q_{\rho,i} \tag{2.1}$$

$$\nabla \cdot \left(\rho \vec{u}\vec{u} + (P_{SW} + P_{PUI} + P_{ACR} + P_{GCR}) \overleftrightarrow{I} \right) = \vec{Q}_p \tag{2.2}$$

$$\nabla \cdot \left(\rho \vec{u} \left\{ \frac{U^2}{2} + \frac{\gamma}{\gamma - 1} \frac{1}{\rho} (P_{SW} + P_{PUI}) \right\} + \vec{F}_{CR} \right) = Q_e \tag{2.3}$$

where $\rho = \rho_{SW} + \rho_{PUI}$ denotes the total mass density of the mixed fluids, $\vec{u}$ the solar wind velocity, $\overleftrightarrow{I}$ the unit tensor, and the quantities P_{SW}, P_{PUI}, P_{ACR}, P_{GCR} the pressures of the solar wind protons, the PUIs, the ACRs and the GCRs, respectively. The polytropic index $\gamma = 5/3$ is taken to be valid for protons and PUIs as well, and the quantities $Q_{\rho,i}, \vec{Q}_p, Q_e$ denote mass-, momentum-, and energy exchange rates per unit volume and time ($i = SW, PUI$). The contribution to the energy flow of the coupled ACRs and GCRs is separately denoted by $\vec{F}_{CR} = \vec{F}_{ACR} + \vec{F}_{GCR}$ and is itself given by the following equations:

$$\vec{F}_{ACR} = \frac{\gamma_{ACR}}{\gamma_{ACR} - 1} \vec{u} P_{ACR} - \frac{\kappa_{ACR}}{\gamma_{ACR} - 1} \nabla P_{ACR} \tag{2.4}$$

$$\vec{F}_{GCR} = \frac{\gamma_{GCR}}{\gamma_{GCR} - 1} \vec{u} P_{GCR} - \frac{\kappa_{GCR}}{\gamma_{GCR} - 1} \nabla P_{GCR} \tag{2.5}$$

where $\gamma_{ACR,GCR} = 4/3$ and $\kappa_{ACR,GCR}$ are the polytropic indices of the high-energy CR-components and the energy-averaged CR spatial diffusion coefficient, respectively. Both ACRs and GCRs are treated as massless fluids by separate energy-averaged particle transport equations. The coupling of these massless fluids occurs because of convective interactions of the CR fluids with the background plasma, inducing a modification of the plasma flow by ACR and GCR pressure gradients.

The required consistency within this model must also include the dynamical and thermodynamical coupling of the mentioned four species to one more

Table 9.1. The heliocentric distances r_i and the compression ratios s_i of the TS in the upwind (u), crosswind (c), and downwind (d) direction ($i = \{u, c, d\}$) for four LISM number densities n_H. The radial velocity profile is approximated by $v(r) \approx v_0 \left(\frac{r_0}{r}\right)^\alpha$ such that at the inner boundary r_0 the radial solar wind speed $v_0 = 400$ km/s. v_u is the velocity just upstream from the TS in upwind direction.

n_H cm^{-3}	r_0 AU	v_u km/s	α	r_u AU	s_u	r_c AU	s_c	r_d AU	s_d	r_u/r_d
0.1	5.1	366.3	0.03	78.3	3.5	107.6	2.2	148.2	2.9	0.53
1.0	5.1	258.4	0.22	32.6	1.6	44.0	1.4	63.6	1.6	0.51
50.0	0.5	286.8	0.12	9.1	1.7	12.5	1.5	17.4	2.1	0.52
100.0	0.5	348.6	0.07	4.0	2.3	6.7	2.1	11.8	3.3	0.34

species, namely the H-atoms. In the Bonn model we treat the H-atoms as an additional hydrodynamical fluid coupled by charge exchange reactions to protons and PUIs. The complete modelling within a two-dimensional multifluid simulation is explained in detail by Fahr (2000) and Fahr et al. (2000), the so-called five-species Bonn model.

9.2.2 Results Obtained with the Bonn Model

In the five-species Bonn model, various parameters have to be specified, for a thorough discussion see Scherer & Fahr (2003). It would go far beyond the scope of this article to study the behavior of the heliosphere under the variation of all parameters. We will rather restrict our modelling to a series of values for the hydrogen density n_H being representative for DISEs along the solar galactic orbit. While it is not quite realistic to keep all other parameters constant, particularly the temperature, it nonetheless is a reasonable approximation, because for all considered model runs the external ram pressure exceeds the thermal pressure significantly. Therefore, reducing the interstellar temperature to ensure a pressure equilibrium in the ISM has no significant consequences for the dynamics of the TS and the heliopause. We consider the values for n_H listed in the first column of Table 1 will refer to the case $n_H = 0.1$ cm^{-3} as the "standard model".

In Fig. 9.1 we show the resulting radial profiles of the radial proton speed, the hydrogen number density, the PUI number density, and the energy density of the ACRs in the upwind direction.

Inspection of Fig. 9.1(d) illustrates how the TS moves inward with increasing interstellar hydrogen density. For the upwind, crosswind, and downwind direction the resulting heliocentric TS distances are listed in Table 1, along with the corresponding compression ratios. At a first glance, astonishingly, the compression ratio is not monotonously decreasing, but increases again for very high

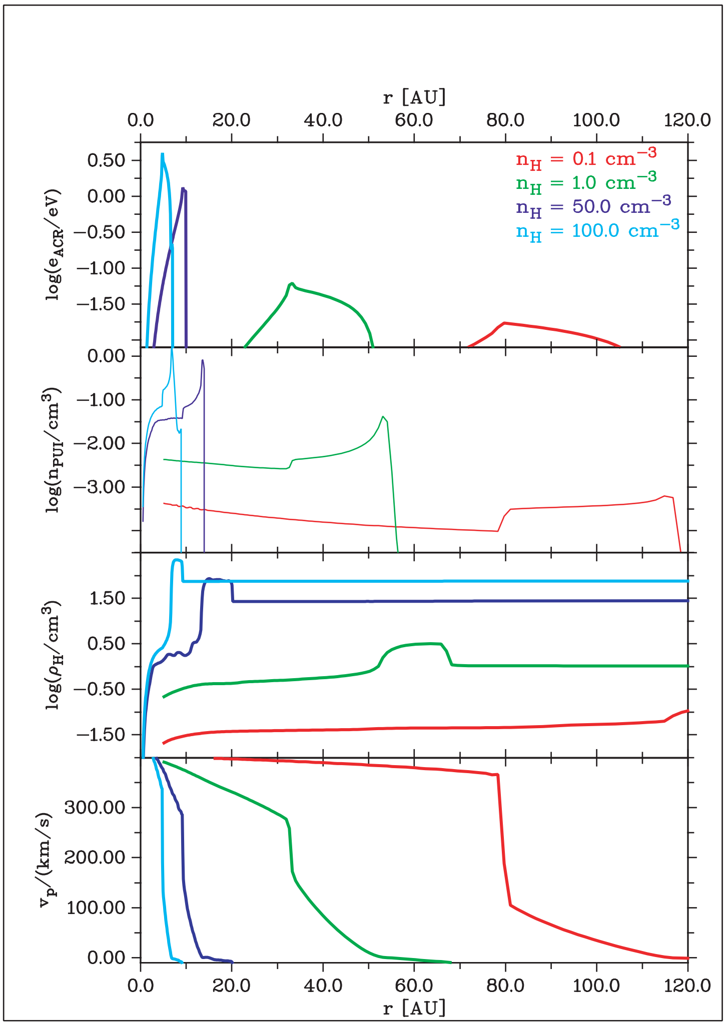

Figure 9.1. Shown from top to bottom are: (a) the ACR energy density, the number densities of the PUIs (b), and the number densities of the neutral hydrogen (c), as well as (d) the proton radial velocity. The red, green, dark blue, and light blue lines represent hydrogen number densities of $n_H = 0.1$, 1.0, 50 and 100 cm^3, respectively.

n_H. This is consistent with the same behaviour of the upstream speed. The reason for this counter-intuitive increase of both is that the net decrease in speed is limited by the short distance to the TS. Therefore, despite the strong momentum loading-induced deceleration resulting from the high hydrogen number density, the solar wind remains fast upstream causing a stronger shock.

Figure 9.1(c) shows that, as expected, the hydrogen density increases at all distances with the hydrogen wall moving inward. Note that the relative strength of the hydrogen wall roughly remains unchanged. It is defined as the maximum value of the hydrogen density inside the bow shock divided by the value at infinity, which is identical to that at the integration boundary and varies by a factor of two between the maximum ($n_H = 0.5\,\mathrm{cm}^{-3}$) and the minimal case ($n_H = 0.1\,\mathrm{cm}^{-3}$), while the cases $n_H = 50$ and $100\,\mathrm{cm}^{-3}$ are close to the value at $n_H = 0.5\,\mathrm{cm}^{-3}$. As a consequence of the increased neutral atom density, the atmospheres of the planets are not only exposed to an enhanced hydrogen influx (Bzowski et al., 1996, Yeghikyan and Fahr, 2004a, Yeghikyan and Fahr, 2004b), but could be located outside the heliopause (see also Begelmann and Rees, 1976, Scherer, 2000),

The heliopause can be nicely seen in panel (b) of Fig. 9.1 at the position where the PUI number density shows a cutoff towards the interstellar medium. Obviously, the PUI density is increased for DISEs. Astonishingly, the ACR energy density shown in panel (a) follows the PUI density increase, although the compression ratio of the TS and, thus, the injection efficiency of PUIs into the process of diffusive shock acceleration varies significantly. The ACR energy density (normalized to that of the standard model) is displayed in Fig. 9.2 and reveals a nonlinear increase with increasing hydrogen number density.

Evidently, the ACR energy density increases by a factor of about 250 from the model with the lowest hydrogen number density compared to that with the highest. Moreover, the peak of the ACR energy density migrates inwards with increasing n_H to about 4 AU.

With the compression ratio, the velocity field, and the size of the heliosphere representing the modulation region (see Table 1), we can compute the associated heliospheric cosmic ray spectra as is done in the following section.

9.3 Cosmic Ray Spectra

Ideally, one would need a self-consistent 'hybrid model' that, on the one hand, describes the (hydro-)dynamics of the heliosphere embedded in the local interstellar medium and, on the other hand, allows for a kinetic treatment of the cosmic ray transport. Several models have been presented that treat either the cosmic ray transport or the heliopheric structure in terms of rather over-simplifying approximations (see, e.g. Myasnikov et al., 2000, Alexashov et al.,

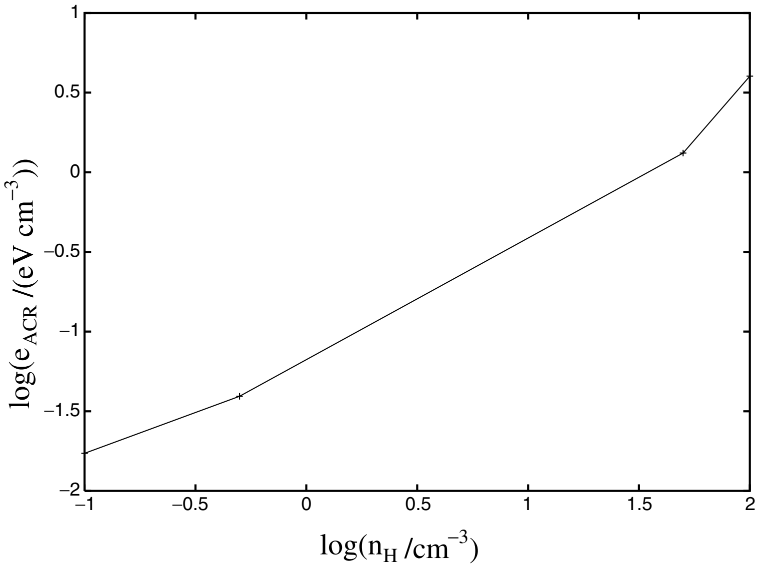

Figure 9.2. The logarithm of normalized ACR energy density e_{ACR} at the TS as a function of the logarithm of the interstellar hydrogen density.

2004), who developed a hybrid description regarding the neutral atoms but used a constant diffusion coefficient, or Florinski et al. (2004), who approximated the heliosheath by a spherical shell.

There are just a few approaches that incorporate both the cosmic ray transport and heliospheric structure in a more advanced fashion. Predecessors to hybrid models in the above sense were studied by Fahr et al. (2000), Scherer & Fahr (2003), and Sreenivasan & Fichtner (2001). While the first two studies are self-consistent two-dimensional fluid models that describe hydrodynamically all considered species (solar and interstellar plasma, neutral gas, pick-up ions, anomalous and galactic cosmic rays), the third study is a first attempt to solve the (steady-state) cosmic ray transport equation including drifts and anisotropic diffusion in a realistic three-dimensionally structured heliosphere.

The first hybrid models describing the cosmic ray transport kinetically everywhere in a "realistic" heliosphere were presented by Florinski et al. (2003), Ferreira et al. (2004), and Ferreira & Scherer (2004). While Florinski et al. concentrated on a partially self-consistent dynamics but neglected drifts, Ferreira et al. and Ferreira and Scherer included fully the drift and diffusion of the cosmic rays, but assumed a substantially simplified dynamics of the heliosphere.

So far, we are still missing a truly dynamical 3-D model for the large-scale heliosphere that includes self-consistently a sophisticated cosmic ray transport comprising anisotropic diffusion and drifts. However a 2-D version has been developed very recently by Scherer & Ferreira (2005). Because this code is still under development, we follow here a different strategy to compute the cosmic rays spectra.

To determine the latter, we employ the semi-analytic model developed by Stawicki et al. (2000), with which, for given solar wind velocity profile ($v(r) \sim r^{-\alpha}$), compression ratio s, and heliocentric distance of the modulation boundary, we estimate the modulated cosmic ray spectra. Note, however, that this is only used to estimate the CR spectra, while the full CR pressure is self-consistently included in the Bonn model as described above.

9.3.1 Boundary Spectra

In order to solve the complete modulation problem, i.e. to compute the spectra of ACRs and GCRs at any location in the heliosphere, we need the ACR and GCR spectra at the boundary of the modulation region. For simplicity, we assume this boundary to be identical with the TS (see Table 1), i.e. neglecting any so far unobserved (but presently discussed) modulation in the inner heliosheath between the TS and the heliopause.

Anomalous Cosmic Rays. It is the general consensus that ACRs result from diffusive acceleration of PUIs at the TS. Therefore, the accelerated spectra are power laws $f \sim p^{-q}$ in the relativistic particle momentum $p = \gamma\, m\, v$, where $q = 3s/(s-1)$ is a function of the compression ratio s, and v is the particle speed. These spectra are normalized such that at low energies they match the PUI spectrum ensuring that the associated energy density

$$e_{ACR} = \frac{p_{ACR}}{\gamma_{ACR} - 1} = \frac{4\pi}{3(\gamma_{ACR} - 1)} \int_0^\infty f\, v\, p^3 dp \qquad (3.1)$$

with $4/3 \leq \gamma_{ACR} \leq 5/3$ is consistent with that computed with the Bonn model (see Fig. 9.2). At high energies there is an exponential cut-off due to the curvature of the TS. The ACR spectra resulting for the four cases listed in Table 1 are shown in Fig. 9.3, where the ACR spectra in the region dominated by the present-day GCR contribution are indicated by the dotted lines. For the present-day interstellar GCR spectrum (see the dotted line below 1 MeV and the solid line above 100 MeV) we have used a standard representation, for a compilation see, e.g., Mori (1997) or Stawicki et al. (2000).

The ACR spectra have a steepening slope as expected for decreasing compression ratio s (see Table 1). At the same time the differential intensity is increased linearly with the interstellar neutral atom number density n_H. The underlying picture here is that the PUI flux is proportional to n_H and that the ACR spectra match the PUI spectra at 1 keV, so that the energy densities

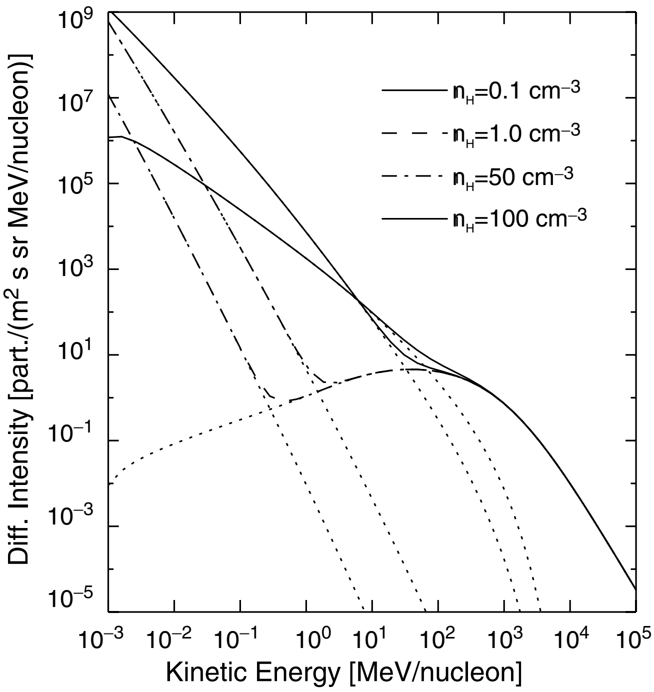

Figure 9.3. The unmodulated ACR spectra at the boundary of the modulation region for present-day conditions (solid line) or inside DISEs. The dotted lines indicate the ACR spectra in the region where GCRs dominate the total flux. For the latter the present-day spectrum is assumed.

corresponding to the computed ACR spectra correspond to those shown in Fig. 9.1. Obviously, only in the case of very dense interstellar environments can the intensity decrease (resulting from the steepening of the spectra) be (over-) compensated by the general increase due to the increased PUI flux: for the two cases $n_H = 1$ and $50\,cm^{-3}$ the ACR intensity dominates the total spectrum only below 1 and 10 MeV, respectively. As modulation will further decrease these fluxes significantly, the resulting intensity at 1 AU is even below the present-day intensity (see Fig. 9.4). From the latter figure, it is evident that only interstellar neutral atom densities of $n_H > 50\,cm^{-3}$ lead to a noticeable intensity increase at 1 AU, i.e. that the decrease of the heliospheric modulation region does not compensate for the steepening of the spectra for lower values. This finding is in agreement with the study by Florinski et al. (2003), who studied the case of a tenfold increase of the ACR intensities and showed that, at Earth, they remain below the GCR intensities at all energies. Therefore, in the following we concentrate on the two cases $n_H = 0.1\,cm^{-3}$ ("present-day") and $n_H = 100\,cm^{-3}$ ("DISE").

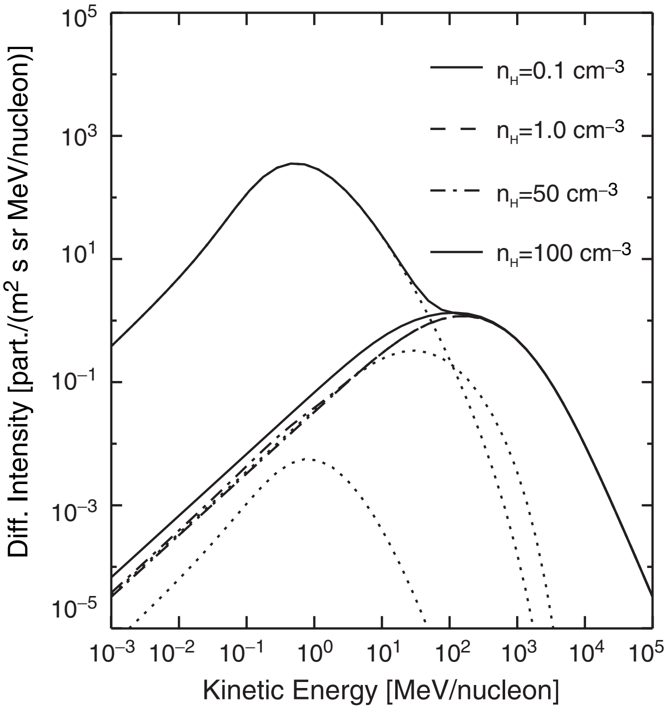

Figure 9.4. The modulated ACR spectra at 1 AU for present-day conditions (solid line) and for DISEs. The dotted lines indicate the ACR spectra in the region where GCRs dominate the total flux. For the latter the present-day spectrum is assumed. Note that the vertical scale has been changed compared to Fig. 9.3.

Galactic Cosmic Rays. While the present-day unmodulated interstellar GCR spectrum in the vicinity of the heliosphere can be derived from observations (for a compilation, see Mori, 1997), the GCR spectra elsewhere can only be obtained from theoretical considerations. It has been demonstrated that there is, at a given position in the Galaxy, a time variation in the spectra of various GCR species resulting from randomly distributed supernova explosions (Büsching et al., 2003). These supernovae represent localized acceleration sites of GCRs with different characteristics essentially resulting in a variation of the spectral indices of the GCR energy spectra at these sources. In addition to this "statistical" variation, one should expect a "regular" variation of the cosmic ray spectra due to the structure of the Galaxy. One of its main features are the spiral arms.

In general, the arms of spiral galaxies are considered to be a result of density waves driven in the galactic plane by an inner bar-like perturbation of the galactic gravitational field, i.e. of the responsible galactic mass distribution. For the Galaxy it is expected that four symmetrically placed spiral arms are developed. They extend from the inner (4/1) and the outer (1/4) Lindblad resonances of Keplerian periods with the corotation period of the bar-like field perturbation (Binney and Tremaine, 1988, Taylor and Cordes, 1993). Not only are these spiral arm regions of condensed galactic (i.e. interstellar matter) often appearing as frequent and dense interstellar clouds, but they also represent regions of an enhanced star formation, of enhanced average electron densities because of abundant HII regions, and of enhanced magnetic fields with a pattern essentially conformal with the density pattern.

The notion that enhanced star formation, for a typical initial mass function, naturally leads to enhanced production rates of massive O-, and B-stars, which then result in supernova events after comparatively short main sequence periods (about 10 to 15 Myr according to Taylor and Cordes, 1993), suggests that spiral arms constitute sites of enhanced supernovae activity and, thus, of enhanced GCR production. Besides, this structure in the source distribution of GCRs, it is also plausible that the diffusive propagation of GCRs is different inside galactic spiral arms as a consequence of both the enhanced magnetic fields, as well as the enhanced turbulence generation created by supernova shock waves. This led to the idea to study the variation of the GCR flux along the galactic orbit of the Sun through arms and interarm regions (Shaviv, 2003). A comparison of the GCR intensities inside and outside spiral arms, envisioning these arm regions as sites of increased star formation, density, and magnetic fields, results in the finding that the GCR flux at the heliospheric modulation boundary exhibits a regular variation with a quasi-period of about 140 Myr, on the basis of an energy-independent spatial diffusion model applied in the well known leaky-box approximation. A study of the cosmic ray exposure age of iron meteorites, as well as the ^{18}O to ^{16}O-isotope ratio in fossils formed in tropical oceans, seem to confirm that such a quasi-period really exists (Shaviv, 2003, Shaviv and Veizer, 2003). The latter correlation, in particular, establishes the strong cosmic ray-climate link mentioned above.

As we are mainly interested in the ACRs, we postpone a more detailed investigation of the GCR flux variation and adopt the general finding that the GCR flux can increase up to a factor of five compared to the present-day value. Therefore, we select two typical cases: first, the established present-day spectrum (for suitable parametrizations, see le Roux & Fichtner (1997) or Stawicki et al. (2000) and, second, a spectrum with five times higher spectral intensities being representative for the inside of a galactic spiral arm (Shaviv, 2003).

All unmodulated total boundary spectra under consideration are displayed in Fig. 9.5. The solid line gives the present-day total spectrum and the dash-dotted line shows the result for an increased ACR intensity in a DISE within a spiral

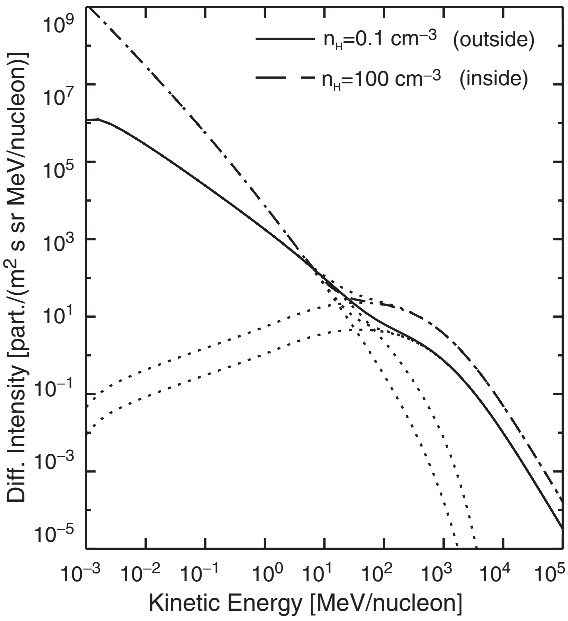

Figure 9.5. The unmodulated ACR and GCR spectra at the boundary of the modulation region for present-day conditions outside clouds or spiral arms and for conditions inside both.

arm leading to a higher GCR flux. The remaining combinations are indicated by the dotted lines.

9.3.2 Modulated Total Spectra at 1 AU

The differential intensity $j = f(\vec{r}, \vec{p}, t)\, p^2$ of cosmic rays with momentum $\vec{p}$ at a location $\vec{r}$ inside the modulation boundary can be estimated using a semi-analytical solution of their phase-space transport equation

$$\frac{\partial f}{\partial t} = \nabla \cdot (\overleftrightarrow{\kappa} \nabla f) - \vec{u} \cdot \nabla f + \frac{1}{3}\,(\nabla \cdot \vec{u})\frac{\partial f}{\partial \ln p} + S(\vec{r}, \vec{p}, t) \tag{3.2}$$

where $\overleftrightarrow{\kappa}$ and $\vec{u}$ denote the diffusion tensor of energetic particles and the solar wind velocity, respectively, and $S(\vec{r}, \vec{p}, t)$ is an injection source. Drift motions are neglected.

By assuming spherical symmetry, and assuming power laws for the dependence of the spatial diffusion coefficient on both heliocentric distance and momentum, as well as for the dependence of the solar wind speed on heliocentric distance (see the caption of Table 1), we can derive the general steady-state solution in the following form (Stawicki et al., 2000):

$$j(r,p) = p^2 f(r,p) = \frac{3}{b}\int dr_0 \int dp_0 \frac{S(r_0,p_0)}{u(r_0)}\frac{p_0 y_0}{F}$$
$$\times\, (r_0/r)^{\frac{1+\beta}{2}} (p_0/p)^{\frac{3\beta-4\alpha-5}{2(2+\alpha)}} \exp\left(-y_0(1+h^2)/F\right)$$
$$\times\, I_{\frac{1+\beta}{1+\alpha-\beta}} (2y_0 h/F) \tag{3.3}$$

which requires a numerical evaluation for non-trivial, i.e. physically realistic sources $S(r_0, p_0)$. The quantity y_0 denotes the so-called modulation parameter, $F = 1 - (p/p_0)^{\frac{3\nu}{2+\alpha}}$; $h = (r/r_0)^{\frac{1+\alpha-\beta}{2}} (p/p_0)^{\frac{3}{2b}}$, I_n is a modified Bessel function of the first kind, $b = (2+\alpha)/(1+\alpha-\beta)$ and $\nu = (1+\alpha-\beta+\frac{2+\alpha}{3}\eta)$. The variables α and β are parameters describing the radial dependence of the solar wind speed and spatial diffusion coefficient, respectively, and η is the dependence of the latter on particle momentum.

While the assumed spherical symmetry of the solution limits its applicability to regions close to a given direction, which we chose as the upwind direction, it nevertheless allows us to estimate the basic changes in the cosmic ray flux levels as function of heliospheric distance r. This way, we obtained the 1 AU spectra displayed in Fig. 9.6.

As in Fig. 9.5 the solid line gives the present-day total spectrum, the dash-dotted line shows the result for an increased ACR intensity in a DISE within a spiral arm, leading to a higher GCR flux, while the other combinations are indicated by the dotted lines. One can clearly see that an n_H-increase associated with a DISE affects the total spectrum for energies below about 50 MeV, while for higher energies a DISE-associated change of the interstellar GCR spectrum is not very important. Note that this conclusion will change for very dense interstellar environments with $n_H > 1000\,\mathrm{cm}^{-3}$, which are typical for molecular clouds. Models for such cases are not as straightforward as, under these conditions, the surrounding medium is dominated by molecular rather than atomic hydrogen, and consequently the interaction scenario might be substantially changed (Yeghikyan and Fahr, 2004a).

9.4 Consequences of Variable Particle Environments

9.4.1 Outer Heliosphere

Obviously, the structure of the whole heliospheric interface adapts to an altered interstellar environment. While nowadays valuable information about this interface region can be extracted from the fluxes of energetic neutral atoms

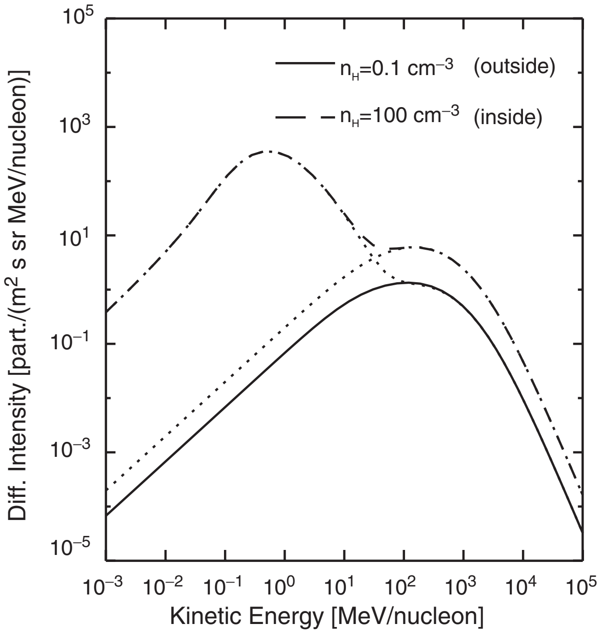

Figure 9.6. The modulated total spectra at 1 AU for $n_H = 0.1\,\mathrm{cm}^{-3}$ and $n_H = 100\,\mathrm{cm}^{-3}$. Note that the vertical scale has been changed as compared to Fig. 5.

(ENAs), which are produced by charge exchange processes between hydrogen atoms and solar wind protons, as well as from PUI protons (Hsieh et al., 1992, Gruntman, 1997), this information would not necessarily be available in cases with different inner and outer boundary conditions. With the Interstellar Boundary Explorer (IBEX), a new space mission is coming up (McComas et al., 2004) that uses the fact that valuable details of the heliospheric structures are reflected in spectral ENA fluxes at Earth for present-day conditions.

In fact, it can be stated that the most valuable information about the present structure of the outer heliosphere comes from the ENA fluxes, which are produced downstream of the termination shock by charge exchange processes of H-atoms with shocked solar wind protons at comparatively low energies ($<$5 keV). In a highly dynamic heliosphere, as characteristic for the present one with its 11-year solar activity cycle, the contribution to the ENA fluxes produced by pick-up protons upstream and downstream of the termination shock are significant only at higher energies greater than 10 keV (Fahr and Scherer, 2004). There is no ENA flux observable at Earth connected with particles originating from upstream solar wind protons, since their velocity vectors responsible for the corresponding ENA velocity vector is almost always directed away from the Sun (supersonic solar wind).

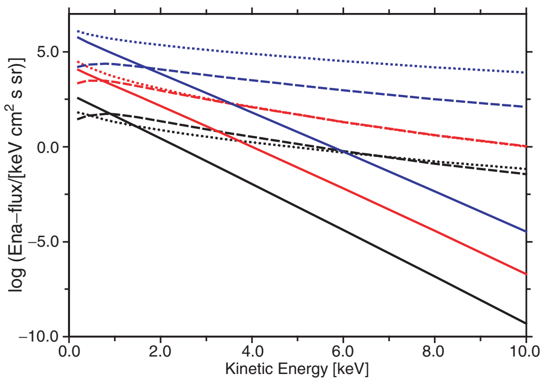

Figure 9.7. The ENA fluxes at 1 AU for $n_H = 0.1,5.0$, and $100\,\mathrm{cm}^{-3}$ produced by the downstream solar wind protons (solid lines) and by the downstream (dashed lines) and upstream (dotted lines) PUI protons. The lowest/highest line in each set corresponds to the lowest/highest hydrogen density in the LISM.

During extended periods of low solar activity (like extended grand minima) the situation is of course different. For quasistatic heliospheric conditions, Figure 9.7 shows the ENA fluxes of the three relevant contributing seed populations (shocked solar wind protons, upstream and downstream PUIs), for some of the DISE cases given in Table 1, and computed for a quasi-static heliosphere from the expression:

$$\Psi(\vec{r},\vec{v}) = \sum_{i=1}^{3} \Psi_i(\vec{r},\vec{v}) = \sum_{i=1}^{3} |n_{\mathrm{i}} f_{\mathrm{i}}(\vec{v}) n_{\mathrm{H}} \sigma_{\mathrm{ex}}(v_{\mathrm{rel}}) v_{\mathrm{rel}}(v)|_{\vec{r}} \qquad (4.1)$$

Here, n_{i} and n_{H} are the number densities of the local protons (i $=$ 1: SW downstream; i $=$ 2: PUIs downstream; i $=$ 3: PUIs upstream) and of the H-atoms, respectively, $f_{\mathrm{i}}(\vec{v})$ is the velocity distribution function, σ_{ex} is the charge exchange cross section, and $v_{\mathrm{rel}}(v)$ is the mean relative velocity between H-atoms and the ions with velocity $\vec{v}$. For further details see Fahr & Scherer (2004).

Evidently, the ENA flux produced by the solar wind protons downstream of the termination shock increases with increasing hydrogen number density (see the solid lines in Fig. 9.7), which also holds true for the ENA fluxes due to the other two seed populations. Closer inspection of Eq. 4.1, however, reveals that these increases are nonlinear. Different from the dynamic present-day situation, the latter two dominate the total flux for all hydrogen number densities at nearly all energies. Under these circumstances the sensitivity of the total ENA flux to the interface structure depends on the relative contribution from upstream and downstream PUIs. Note, however, that the situation will change in a dynamical heliosphere governed by variable solar wind momentum flows, triggered by the solar activity cycle as described by Fahr and Scherer (2004).

9.4.2 Solar System Bodies

In the following we discuss the consequences of an increase of the cosmic ray intensities below about 50 MeV due to the enhanced production of ACRs.

Earth. The terrestrial atmosphere is influenced mostly by cosmic ray particles in the energy range 0.1-1 GeV (see the discussion in Scherer, 2000, Scherer et al., 2002), because for lower energies the particles cannot penetrate deep enough through the Earth' magnetosphere into the atmosphere and for higher energies the total flux is too low. Figure 9.6 reveals that, at least for DISE with $n_H \leq 100\,\mathrm{cm}^{-3}$, one should not expect any significant influence of ACRs on the atmosphere and, in particular, on the terrestrial climate as is discussed for GCRs (Svensmark, 1998, Svensmark, 2000 or Shaviv and Veizer, 2003). As mentioned above, this might change for very dense interstellar environments that, however, cannot be modelled with the current model.

As an aside, we mention that the discussion of whether, and if, cosmic rays at all energies could influence the terrestrial climate has just begun. It might turn out that the upper layer of the stratosphere plays an essential role in the long-term behavior of the terrestrial climate through its high altitude clouds. Also, the lower energetic cosmic rays like ACRs can penetrate to such high altitudes. Relevant work on this whole new context is just under discussion, and a more quantitative discussion should be possible in the near future (for example in the forthcoming special issue of Adv. Space Research on the “Influence of the Sun’s Radiation and Particles on the Earth’s Atmosphere and Climate”, edited by J. Pap).

Planets. While the cosmic ray-climate connection might not be affected for cases of a heliosphere immersed in a DISE, there is still another potentially important effect. Within a DISE, not only do PUI or ACR fluxes increase but, of course, also the direct flux of low energy neutral atoms (LENA’s). As hydrogen easily chemically reacts with most constituents of planetary atmospheres, these atmospheres can be significantly affected by such a flux increase (see Bzowski et al., 1996, Yeghikyan and Fahr, 2004a, Yeghikyan and Fahr, 2004b). This effect can be amplified for the outer planets, which might be located outside the reduced dimensions of the heliosphere and, thus, be directly in contact with the LISM. In that case the structure of the planetary magnetospheres will also be affected.

Small bodies. Especially those objects which do not have an atmosphere or magnetosphere are directly influenced by the ACR radiation, potentially dominating the fluxes at intermediate and low energies. The top layer of the surfaces of the outer planetary moons can be chemically influenced, as well as the objects from the Kuiper Belt. In DISEs, Kuiper Belt objects will move most likely in orbits located beyond the termination shock, and are thus immersed in the local interstellar medium, while the planetary moons are exposed to an enhanced ACR flux. The cosmic ray bombardment of their surfaces alters the matrix of the minerals and is an additional explanation for the different albedo of these objects. The same holds true for cometary dust and Polycyclic Aromatic Hydrocarbons (PAHs).

Unfortunately, the meteorites found on Earth undergo an ablation process during their passage through the atmosphere and lose parts of their surface. Therefore, they are not good tracers for the cosmic ray radiation history. The surface of the Moon may also be a poor tracer, because the signatures of cosmic rays have to be disentangled from those of the solar wind and of solar energetic particles. With future missions, it might become possible to detect meteorites on the Moon that are not ablated, so that their surface mineralogy may serve as a tracer for the cosmic history of the solar system.

References

Alexashov, D. B., Chalov, S. V., Myasnikov, A. V., Izmodenov, V. V., Kallenbach, R., The dynamical role of anomalous cosmic rays in the outer heliosphere, Astron. Astrophys. 420, 729, 2004

Begelmann, M. C. and Rees M. J., Can cosmic clouds cause climatic catastrophes?, Nature 261, 298–299, 1976

Binney, J., Tremaine, S., *Galactic Dynamics*, Princeton University Press, 1988

Breitschwerdt, D., Self-consistent Modelling of the interstellar medium, Astrophys. Space Sci. 289, 489–498, 2004

Büsching, I., Kopp, A., Pohl, M., Schlickeiser, R., First results of a new cosmic ray propagation code, 28th Int. Cosmic Ray Conf., Tsukuba, Japan, OG, 1981–1984, 2003

Bzowski, M., Fahr, H. J., Rucinski, D., Interplanetary Neutral Particle Fluxes Influencing the Earth's Atmosphere and the Terrestrial Environment, Icarus, 124, 209–219, 1996

Caballero-Lopez, R. A., Moraal, H., McCracken, K. G., McDonald, F. B., The heliospheric magnetic field from 850 to 2000 AD, submitted

Carslaw, K. S., Harrison, R. G., Kirkby, J., Cosmic Rays, Clouds, and Climate, Science 298, 1732–1737, 2002

Chalov, S. V. and Fahr, H. J., A two-fluid model of the solar wind termination shock modified by shock-generated cosmic rays including energy losses, Astron. Astrophys., 288, 973–980, 1994

Chalov, S. V. and Fahr, H. J., The Multifluid Solar Wind Termination Shock and its Influence on the Three-dimensional Plasma Structure Upstream and Downstream, Space Sci. Rev., 72, 237, 1995

Chalov, S. V. and Fahr, H. J., The three-fluid structure of the particle modulated solar wind termination shock, Astron. Astrophys., 326, 860–869, 1997

Cuntz, M., von Bloh, W., Bounama, C., Franck, S., On the possibility of Earth-type habitable planets around 47 UMa, Icarus 162, 214–221, 2003

Fahr, H.-J., Formation of the heliospheric boundaries and the induced dynamics of the solar system: a multifluid view, In: The outer heliosphere: beyond the planets. Based on the spring school "Die äußere Heliosphäre - Jenseits der Planeten," Bad Honnef, Germany, 12-16 April 1999, Eds.: K. Scherer, H. Fichtner, E. Marsch, Katlenburg-Lindau, Germany, Copernicus-Gesellschaft., 67–89, 2000

Fahr, H. J., Scherer, K., Energetic neutral atom fluxes from the heliosheath varying with the activity phase of the solar cycle, ASTRA, 1, 3–15, 2004

Fahr, H. J., Kausch, T., Scherer, H., A 5-fluid hydrodynamic approach to model the solar system-interstellar medium interaction, Astron. Astrophys., 357, 268–282, 2000

Ferreira, S. E. S., Scherer, K., Modulation of Cosmic-Ray Electrons in the Outer Heliosphere, Astrophys. J., 616, 1215–1223, 2004

Ferreira, S. E. S., Potgieter, M. S., Scherer, K., Modulation of Cosmic-Ray Electrons in a Nonspherical and Irregular Heliosphere, Astrophys. J., 607, 1014, 2004

Florinski, V, Zank, G. P., Axford, W. I., The Solar System in a dense interstellar cloud: Implications for cosmic-ray fluxes at Earth and 10Be records, Geophys. Res. Lett., 30, 2206, 2003

Florinski, V., Zank, G. P., Jokipii, J. R., Stone, E. C., Cummings, A. C., Do Anomalous Cosmic Rays Modify the Termination Shock?, Astrophys. J., 611, 1169, 2004

Freyberg, M. J., Breitschwerdt, D. XMM-Newton local bubble and galactic halo survey, Astron. Nach. 324, 162, 2003

Frisch, P. C., Interstellar Matter and the Boundary Conditions of the Heliosphere, Space Sci. Rev., 86, 107–126, 1998

Fröhlich, C., Lean, J., Solar irradiance variability and climate, Astron. Nach., 323, 203–212, 2002

Gruntman, M., Energetic neutral atom imaging of space plasmas, Rev. Sci. Inst., 68, 3617–3656, 1997

Hsieh, K. C., Shih, K. L., Jokipii, J. R. and Grzedzielski, S., Probing the heliosphere with energetic hydrogen atoms, Astrophys. J., 393, 756–763, 1992

Lallement, R., Welsh, B. Y., Vergely, J. L., Crifo, F., Sfeir, D., 3D mapping of the dense interstellar gas around the Local Bubble, Astron. Astrophys., 411, 447–464, 2003

Lean, J., Rind, D., Evaluating Sun-climate relationships since the Little Ice Age, J. Atmos. Sol.-Terr. Phys., 61, 25–36, 1999

le Roux, J. A., Fichtner, H., A self-consistent determination of the heliospheric termination shock structure in the presence of pick-up, anomalous, and galactic cosmic ray protons, J. Geophys. Res., 102, 17365–17380, 1997

McComas, D., Allegrini, F., Bochsler, P., Bzowski, M., Collier, M., Fahr, H., Fichtner, H., Frisch, P., Funsten, H., Fuselier, S., Gloeckler, G., Gruntman, M., Izmodenov, V., Knappenberger, P., Lee, M., Livi, S., Mitchell, D., Mï¿¿bius, E., Moore, T., Reisenfeld, D., Roelof, E., Schwadron, N., Wieser, M., Witte, M., Wurz, P., Zank, G. P., The Interstellar Boundary Explorer (IBEX) in: Physics of the Outer Heliosphere, AIP Conf. Proc., 719, February 2004, Riverside, California. Eds.: V. Florinski, N. V. Pogorelov, G. P. Zank, American Institute of Physics, 162–181, 2004

Mori, M., The galactic diffuse gamma-ray spectrum from cosmic ray proton interactions, Astrophys. J., 478, 225–232, 1997

Myasnikov, A. V., Izmodenov, V. V., Aleksashov, D. B., Chalov, S. V., Self-consistent model of the solar wind interaction with two-component circumsolar interstellar cloud: Mutual influence of thermal plasma and galactic cosmic rays, J. Geophys. Res., 105, 5179, 2000

Scherer, K., Variations of the heliospheric shield, In: *The Outer Heliosphere: Beyond the Planets*, Eds.: Scherer, K., Fichtner, H., Marsch, E., Copernicus-Gesellschaft., 327–355, 2000

Scherer, K., Fichtner, H., Stawicki, O., Shielded by the wind: the influence of the interstellar medium on the environment of Earth, J. Atmos. Sol.-Terr. Phys. 64, 795–804, 2002

Scherer, K., Fahr, H. J., Solar cycle induced variations of the outer heliospheric structures, Geophys. Res. Lett. 30, 17-1, CiteID 1045, DOI 10.1029/2002GL016073

Scherer, K., Ferreira, S. E. S., A heliospheric hybrid model: hydrodynamic plasma flows and kinetic cosmic ray transports, ASTRA, 1, 17–27

Scherer, K., Fichtner, H., Constraints on the heliospheric magnetic field variation during the Maunder Minimum from cosmic ray modulation modelling, Astron. Astrophys. 413, L11–L14, 2004

Shaviv, N. J., The spiral structure of the Milky Way, cosmic rays, and ice age epochs on Earth, New Astron., 8, 39–77, 2003

Shaviv, N. J., Veizer, J., Celestial driver of Phanerozoic climate?, GSA Today 13, 4–10, 2003

Sreenivasan, S. R., Fichtner, H., ACR modulation inside a non-spherical modulation boundary, in: The Outer Heliosphere: The Next Frontiers, Edited by

K. Scherer et al., COSPAR Colloquia Series, Vol. 11, Amsterdam: Pergamon Press, 207, 2001

Stawicki, O., Fichtner, H., Schlickeiser, R., The Parker propagator for spherical solar modulation, Astron. Astrophys., 358, 347–352, 2000

Svensmark, H., Influence of Cosmic Rays on Earth's Climate, Phys. Rev. Lett., 81, 5027–5030, 1998

Svensmark, H., Cosmic rays and Earth's climate, Space Sci. Rev., 93, 175–185, 2000

Svensmark, H., Friis-Christensen, E., Variation of cosmic ray flux and global cloud coverage–a missing link in solar-climate relationships, J. Atm. Sol. Terr. Phys., 59, 1225–1232, 1997

Taylor, J. H., Cordes, J. M., Pulsar distances and the galactic distribution of free electrons, Astrophys. J. 411, 674–684, 1993

von Bloh, W., Cuntz, M., Franck, S., Bounama, C., On the Possibility of Earth-Type Habitable Planets in the 55 Cancri System, Astrobiology 3, 681–688, 2003

Yeghikyan, A. G., Fahr, H. J., Effects induced by the passage of the Sun through dense molecular clouds. I. Flow outside of the compressed heliosphere Astron. Astrophys. 415, 763–770, 2004a

Yeghikyan, A. G., Fahr, H. J., Terrestrial atmospheric effects induced by counter-streaming dense interstellar cloud material, Astron. Astrophys., 425, 1113–1118, 2004b

Zank, G. P., Interaction of the solar wind with the local interstellar medium: a theoretical perspective, Space Sci. Rev., 89, 413, 1999

Zank, G. P., Frisch, P. C., Consequences of the change in the galactic environment of the Sun, Astrophys. J., 518, 965–973, 1999